

Quantum memory in non-inertial frames

M. Ramzan and M. K. Khan

*Department of Physics Quaid-i-Azam University
Islamabad 45320, Pakistan*

We study the effect of quantum memory in non-inertial frames under the influence of amplitude damping, depolarizing, phase flip and bit-phase flip channels. It is shown that the entanglement of initial state is heavily influenced by quantum correlations. It is seen that quantum memory compensates the loss of entanglement caused by the Unruh effect. It is interesting to note that the sudden death of entanglement disappears for any acceleration for higher values of quantum memory. Therefore, it is possible to avoid ESD in non-inertial frames due to the presence of quantum memory. Furthermore, the degree of entanglement is enhanced as we increase the degree of memory and it maximizes for maximum correlations.

Keywords: Quantum memory; entanglement; quantum channels.

I. INTRODUCTION

Quantum entanglement being a fundamental potential resource for communication is one of the key quantitative notions of the intriguing field of quantum information and quantum computation. Entanglement behavior in non-inertial frames was first considered by Alsing et al. [1]. They studied the fidelity of teleportation between relative accelerated partners. Afterwards, a number of authors have focused on the topic of the quantum information in a relativistic setup [2-8]. Schuller et al. [9] have studied how the Unruh effect changes the degree of quantum entanglement. However, all the investigations in non-inertial frames were confined to the studies of quantum information in an isolated system except [10, 11], where the authors have analyzed the decoherence effects in non-inertial frames.

Since in a realistic quantum system, the interaction between the quantum system and the surrounding environment is inevitable, it is therefore, important to study the effect of environmental influences on the entanglement dynamics of a system. Quantum channels can be implemented by

suitable quantum devices consisting of intrinsic degrees of freedom associated with the environment and acting on the system via particular interactions between the system and the environment. The assumption that noise is uncorrelated between successive uses of a channel is not realistic. Hence memory effects need to be taken into account. Quantum channels with memory [12-14] are the natural theoretical framework for the study of any noisy quantum communication system where correlation time is longer than the time between consecutive uses of the channel. A more general model of a quantum channel with memory was introduced by Bowen and Mancini [15] and also studied by Kretschmann and Werner [16].

In this paper, we investigate the effect of quantum memory on the entanglement of Dirac fields in non-inertial frames. We consider the amplitude damping, depolarizing, phase flip and bit-phase flip channels. We assume that two observers, Alice and Rob, share an entangled initial state at the same point in flat Minkowski spacetime. After that Alice stays stationary while Rob moves with uniform acceleration. We assume that Alice and Rob have detectors that are sensitive only to their respective modes and both the observers share the following maximally entangled initial state

$$|\Psi\rangle_{AR} = \frac{1}{\sqrt{2}} (|0\rangle_A|0\rangle_R + |1\rangle_A|1\rangle_R) \quad (1)$$

where the two modes of Minkowski spacetime that correspond to Alice and Rob are $|\eta\rangle_A$ and $|\eta\rangle_R$ respectively. From the perspective of Rob, the Minkowski vacuum is found to be a two-mode squeezed state [4]

$$|0\rangle_M = \cos r|0\rangle_I|0\rangle_{II} + \sin r|1\rangle_I|1\rangle_{II} \quad (2)$$

where $\cos r = (e^{-2\pi\omega c/a} + 1)^{-1/2}$. The constants ω , c and a , in the exponential stand for Dirac particle's frequency, light's speed in vacuum and Rob's acceleration respectively. The subscripts I and II of the kets represent the Rindler modes in region I and II , respectively, in the Rindler spacetime diagram (see Ref. [10], Fig. (1)). The excited state in Minkowski spacetime is related to Rindler modes as follows [4]

$$|1\rangle_M = |1\rangle_I|0\rangle_{II} \quad (3)$$

Using equations (2) and (3), equation (1) can be written in terms of Minkowski modes for Alice and Rindler modes for Rob as

$$|\Psi\rangle_{A,I,II} = \frac{1}{\sqrt{2}} (\cos r|0\rangle_A|0\rangle_I|0\rangle_{II} + \sin r|0\rangle_A|1\rangle_I|1\rangle_{II} + |1\rangle_A|1\rangle_I|0\rangle_{II}) \quad (4)$$

Since Rob is causally disconnected from region II , therefore, by tracing over all the modes in region II leaves the following mixed density matrix between Alice and Rob

$$\rho_{A,I} = \frac{1}{2} (\cos^2 r |00\rangle \langle 00| + \cos r (|00\rangle \langle 11| + |11\rangle \langle 00|) + \sin^2 r |01\rangle \langle 01| + |11\rangle \langle 11|) \quad (5)$$

We study the entanglement of Dirac fields in non-inertial frames influenced by different memory channels, such as amplitude damping, depolarizing, phase flip and bit-phase-flip channels, parameterized by decoherence parameter p and memory parameter μ . Here $p \in [0, 1]$ and $\mu \in [0, 1]$ represent the lower and upper limits of decoherence parameter and memory parameter respectively. It is seen that depolarizing channel influences the entanglement of Dirac fields heavily in comparison to the amplitude damping and flipping channels. Therefore, the entanglement of Dirac fields is strongly dependent on degree of correlations of the noisy channels.

II. ENTANGLEMENT IN A CORRELATED ENVIRONMENT

Since noise is a major hurdle while transmitting quantum information from one party to other through classical and quantum channels. This noise causes a distortion of the information sent through the channel. If multiple uses of a channel are not correlated, there is no advantage in using entangled states. Correlated noise, also referred as memory in the literature, acts on consecutive uses of the channel. However, in general, one may want to encode classical data into entangled strings or consecutive uses of the channel may be correlated to each other. Hence, we are dealing with a strongly correlated quantum system, the correlation of which results from the memory of the channel itself. In Ref. [12], a Pauli channel with partial memory was studied. The action of such a channel on two consecutive qubits is given in Kraus operator form as

$$A_{ij} = \sqrt{p_i [(1 - \mu)p\alpha_j + \mu\delta_{ij}]} \sigma_i \otimes \sigma_j \quad (6)$$

where σ_i (σ_j) are usual Pauli matrices, p_i (p_j) represent the quantum noise and indices i and j runs from 0 to 3. The above expression means that with probability μ the channel acts on the second qubit with the same error operator as on the first qubit, and with probability $(1 - \mu)$ it acts on the second qubit independently. Physically the parameter μ is determined by the relaxation time of the channel when a qubit passes through it. In order to remove correlations, one can wait until the channel has relaxed to its original state before sending the next qubit, however this lowers the rate of information transfer. Thus it is necessary to consider the performance of the channel for arbitrary values of μ to reach a compromise between various factors which determine the final rate

of information transfer. Thus in passing through the channel any two consecutive qubits undergo random independent (uncorrelated) errors with probability $(1 - \mu)$ and identical (correlated) errors with probability μ . This should be the case if the channel has a memory depending on its relaxation time and if we stream the qubits through it. A detailed list of single qubit Kraus operators for different quantum channels with uncorrelated noise is given in table 1. The action of such a channel if n qubits are streamed through it, can be described in operator sum representation as [17]

$$\rho_f = \sum_{k_1, \dots, k_n=0}^{n-1} (A_{k_n} \otimes \dots \otimes A_{k_1}) \rho_{in} (A_{k_1}^\dagger \otimes \dots \otimes A_{k_n}^\dagger) \quad (7)$$

where ρ_{in} represents the initial density matrix for quantum state and A_{k_n} are the Kraus operators expressed in equation (6). The Kraus operators satisfy the completeness relation

$$\sum_{k_n=0}^{n-1} A_{k_n}^\dagger A_{k_n} = 1 \quad (8)$$

However, the Kraus operators for a quantum amplitude damping channel with correlated noise are given by Yeo and Skeen [13] as given as

$$A_{00}^c = \begin{bmatrix} \cos \chi & 0 & 0 & 0 \\ 0 & 1 & 0 & 0 \\ 0 & 0 & 1 & 0 \\ 0 & 0 & 0 & 1 \end{bmatrix}, \quad A_{11}^c = \begin{bmatrix} 0 & 0 & 0 & 0 \\ 0 & 0 & 0 & 0 \\ 0 & 0 & 0 & 0 \\ \sin \chi & 0 & 0 & 0 \end{bmatrix} \quad (9)$$

where, $0 \leq \chi \leq \pi/2$ and is related to the quantum noise parameter as

$$\sin \chi = \sqrt{p} \quad (10)$$

It is clear that A_{00}^c cannot be written as a tensor product of two two-by-two matrices. This gives rise to the typical spooky action of the channel: $|01\rangle$ and $|10\rangle$, and any linear combination of them, and $|11\rangle$ will go through the channel undisturbed, but not $|00\rangle$. The action of this non-unital channel is given by

$$\pi \rightarrow \rho = \Phi(\pi) = (1 - \mu) \sum_{i,j=0}^1 A_{ij}^u \pi A_{ij}^{u\dagger} + \mu \sum_{k=0}^1 A_{kk}^c \pi A_{kk}^{c\dagger} \quad (11)$$

The action of the super-operators provides a way of describing the evolution of quantum states in a noisy environment. In our scheme, the Kraus operators are of the dimension 2^2 . They are constructed from single qubit Kraus operators by taking their tensor product over all n^2 combinations

$$A_k = \otimes_{k_n} A_{k_n} \quad (12)$$

where n is the number of Kraus operator for a single qubit channel. The final state of the system after the action of the channel can be obtained as

$$\rho_f = \Phi_{p,\mu}(\rho_{A,I}) \quad (13)$$

where $\Phi_{p,\mu}$ is the super-operator realizing the quantum channel parametrized by real numbers p and μ . The density matrix after the action of different memory channels are obtained by using equations (5-13). It is important to mention here that we consider the case that both the qubits are coupled to the time correlated channel with memory. The final density matrix after the action of amplitude damping channel is given by

$$\rho_f^{\text{AD}} = \begin{pmatrix} \frac{1}{2}(-(-1 + \mu)p(1 + p)) & 0 & 0 & \frac{1}{2}(1 - p + \mu(-1 + \sqrt{(1 - p) + p})) \cos r \\ -(-1 + p) \cos^2 r & & & \\ 0 & \frac{1}{2}(1 + (-1 + \mu)p^2 + (-1 + p - \mu p) \cos^2 r) & 0 & 0 \\ 0 & 0 & \frac{1}{2}(-1 + \mu) & 0 \\ & & (-1 + p)p & \\ \frac{1}{2}(1 - p + \mu(-1 + \sqrt{(1 - p) + p})) \cos r & 0 & 0 & \frac{1}{2}(1 - (-1 + \mu) + (-2 + p)p + \mu p \cos^2 r) \end{pmatrix} \quad (14)$$

The final density matrix after the action of depolarizing channel is given by

$$\rho_f^{\text{Dep}} = \begin{pmatrix} \frac{1}{8} \cos^2 r(2 + p(-3 - 2\mu(-2 + p) + 2p)) & 0 & 0 & \frac{1}{16} \cos r(4 + (-2 + \mu)p + (4 + p(-10 + \mu(11 - 6p) + 6p)) \cos^2 r) \\ 0 & \frac{1}{16}(4 + (-2 + \mu)p + 2(-2 + p)(1 + (-1 + \mu)p) \cos^2 r) \sin^2 r & -\frac{1}{16} \mu p \cos r \sin^2 r & 0 \\ 0 & 0 & 0 & 0 \\ \frac{1}{8} \cos r(2 + p(-3 - 2\mu(-2 + p) + 2p)) & 0 & 0 & \frac{1}{16}(4 + (-2 + \mu)p + (4 + p(-10 + \mu(11 - 6p) + 6p)) \cos^2 r) \end{pmatrix} \quad (15)$$

The final density matrix after the action of bit-phase flip channel is given by

$$\rho_f^{\text{Bpf}} = \begin{pmatrix} \frac{1}{4}(1 + p(-1 - 2\mu(-1 + p) + 2p) - (-1 + p)(1 + 2(-1 + \mu)p) \cos(2r)) & 0 & 0 & \frac{1}{16} \cos r(4 + (-2 + \mu)p + (4 + p(-10 + \mu(11 - 6p) + 6p)) \cos^2 r) \\ 0 & \frac{1}{16}(4 + (-2 + \mu)p + 2(-2 + p)(1 + (-1 + \mu)p) \cos^2 r) \sin^2 r & -\frac{1}{16}\mu p \cos r \sin^2 r & 0 \\ 0 & 0 & 0 & 0 \\ \frac{1}{8} \cos r(2 + p(-3 - 2\mu(-2 + p) + 2p) - (-2 + p)(1 + (-1 + \mu)p) \cos^2 r) & 0 & 0 & \frac{1}{16}(4 + (-2 + \mu)p + (4 + p(-10 + \mu(11 - 6p) + 6p)) \cos^2 r) \end{pmatrix} \quad (16)$$

The final density matrix after the action of phase flip channel is given by

$$\rho_f^{\text{Pf}} = \begin{pmatrix} \frac{1}{2} \cos^2 r & 0 & 0 & \frac{1}{2}(1 + 4p(-1 + \mu + p - \mu p)) \cos r \\ 0 & \frac{1}{2} \sin^2 r & -\frac{1}{16}\mu p \cos r \sin^2 r & 0 \\ 0 & 0 & 0 & 0 \\ \frac{1}{2}(1 + 4p(-1 + \mu + p - \mu p)) \cos r & 0 & 0 & \frac{1}{2} \end{pmatrix} \quad (17)$$

where the super-scripts AD, Dep, Bpf and Pf correspond to the amplitude damping, depolarizing, bit-phase flip and phase flip channels respectively. In order to study the degree of entanglement in the two qubits mixed state in a correlated noisy environment we calculate the concurrence C , which is given as [18]

$$C = \max\{0, \sqrt{\lambda_1} - \sqrt{\lambda_2} - \sqrt{\lambda_3} - \sqrt{\lambda_4}\} \quad \lambda_i \geq \lambda_{i+1} \geq 0 \quad (18)$$

where λ_i are the eigenvalues of the matrix $\rho_f \tilde{\rho}_f$, with $\tilde{\rho}_f$ being the spin flip matrix of ρ_f (as given in equations (14-17)) and is given as

$$\tilde{\rho}_f = (\sigma_y \otimes \sigma_y) \rho_f (\sigma_y \otimes \sigma_y) \quad (19)$$

where σ_y is the usual Pauli matrix. The eigen values of $\rho_f^{\text{AD}} \tilde{\rho}_f^{\text{AD}}$ are given as under

$$\begin{aligned}
\lambda_{1,2} &= \frac{1}{4}(p - \mu p - p^2 + 3\mu p^2 - 2\mu^2 p^2 - p^3 + 2\mu p^3 - \mu^2 p^3 + p^4 \\
&\quad - 2\mu p^4 + \mu^2 p^4 + 2 \cos^2 r - 2\mu \cos^2 r + 2\mu^2 \cos^2 r + 2\mu \sqrt{1-p} \cos^2 r \\
&\quad - 2\mu^2 \sqrt{1-p} \cos^2 r - 5p \cos^2 r + 6\mu p \cos^2 r - 3\mu^2 p \cos^2 r - 2\mu \sqrt{1-pp} \cos^2 r \\
&\quad + 2\mu^2 \sqrt{1-pp} \cos^2 r + 4p^2 \cos^2 r - 4\mu p^2 \cos^2 r - p^3 \cos^2 r + 2\mu p^3 \cos^2 r \\
&\quad - \mu^2 p^3 \cos^2 r + \mu p \cos r^4 - \mu p^2 \cos r^4 \\
&\quad \pm \frac{1}{\sqrt{2}} \sqrt{\left(\begin{aligned} &((-1+p)(-1+p-2\mu(-1+\sqrt{1-p}+p) \\ &\quad + \mu^2(-2+2\sqrt{1-p}+p)) \cos^2 r \\ &(4-4p+3\mu p+4p^2+13\mu p^2-20\mu^2 p^2 \\ &-12p^3+24\mu p^3-12\mu^2 p^3+8p^4-16\mu p^4+8\mu^2 p^4 \\ &-4(-1-3(-1+\mu)p+(-3+3\mu+\mu^2)p^2 \\ &\quad +(-1+\mu)^2 p^3) \cos(2r) - \mu(-1+p)p \cos(4r) \end{aligned} \right)} \\
\lambda_{3,4} &= \frac{1}{4}(-1+\mu)(-1+p)p(1+(-1+\mu)p^2+(-1+p-\mu p) \cos^2 r)
\end{aligned} \tag{20}$$

Similarly, the eigen values of $\rho_f^{\text{Dep}} \tilde{\rho}_f^{\text{Dep}}$ are given below

$$\begin{aligned}
\lambda_1 &= \frac{1}{32} \cos^2 r (8 + 2(-8 + 9\mu)p + (14 - 19\mu + 4\mu^2)p^2 \\
&\quad - 2(2 - 3\mu + \mu^2)p^3 + (16 + 48(-1 + \mu)p \\
&\quad + 2(30 - 52\mu + 23\mu^2)p^2 + (-40 + 87\mu - 47\mu^2)p^3 \\
&\quad + 12(-1 + \mu)^2 p^4) \cos^2 r + (-2 + p)(-4 + (14 - 15\mu)p \\
&\quad + (-16 + 27\mu - 11\mu^2)p^2 + 6(-1 + \mu)^2 p^3) \cos r^4) \\
\lambda_{2,3,4} &= 0
\end{aligned} \tag{21}$$

and the eigen values of $\rho_f^{\text{Bpf}} \tilde{\rho}_f^{\text{Bpf}}$ are obtained as

$$\begin{aligned}
\lambda_{1,2} = & \frac{1}{32}(8 - 27p + 30\mu p + 55p^2 - 86\mu p^2 + 28\mu^2 p^2 - 56p^3 \\
& + 112\mu p^3 - 56\mu^2 p^3 + 28p^4 - 56\mu p^4 + 28\mu^2 p^4 \\
& + 8 \cos(2r) - 36p \cos(2r) + 32\mu p \cos(2r) + 68p^2 \cos(2r) \\
& - 96\mu p^2 \cos(2r) + 32\mu^2 p^2 \cos(2r) - 64p^3 \cos(2r) \\
& + 128\mu p^3 \cos(2r) - 64\mu^2 p^3 \cos(2r) + 32p^4 \cos(2r) \\
& - 64\mu p^4 \cos(2r) + 32\mu^2 p^4 \cos(2r) - p \cos(4r) \\
& + 2\mu p \cos(4r) + 5p^2 \cos(4r) - 10\mu p^2 \cos(4r) \\
& + 4\mu^2 p^2 \cos(4r) - 8p^3 \cos(4r) + 16\mu p^3 \cos(4r) \\
& - 8\mu^2 p^3 \cos(4r) + 4p^4 \cos(4r) - 8\mu p^4 \cos(4r) + 4\mu^2 p^4 \cos(4r) \\
& \pm 4\sqrt{2} \sqrt{\left(\begin{aligned} & ((1 + 2(-1 + \mu)p - 2(-1 + \mu)p^2)^2 \cos^2 r(4 - 11p \\ & + 14\mu p + 23p^2 - 38\mu p^2 + 12\mu^2 p^2 \\ & - 24p^3 + 48\mu p^3 - 24\mu^2 p^3 + 12p^4 - 24\mu p^4 \\ & + 12\mu^2 p^4 + 4(1 + (-5 + 4\mu)p + (3 - 2\mu)^2 p^2 \\ & - 8(-1 + \mu)^2 p^3 + 4(-1 + \mu)^2 p^4) \cos(2r) \\ & + (-1 + p)p((1 - 2p)^2 - 2\mu(1 - 2p)^2 + 4\mu^2(-1 + p)p) \cos(4r) \end{aligned} \right)} \\
\lambda_{3,4} = & \frac{1}{32}(5p - 2\mu p + 23p^2 - 54\mu p^2 + 28\mu^2 p^2 - 56p^3 + 112\mu p^3 - 56\mu^2 p^3 \\
& + 28p^4 - 56\mu p^4 + 28\mu^2 p^4 - 4p \cos(2r) + 36p^2 \cos(2r) - 64\mu p^2 \cos(2r) \\
& + 32\mu^2 p^2 \cos(2r) - 64p^3 \cos(2r) + 128\mu p^3 \cos(2r) - 64\mu^2 p^3 \cos(2r) \\
& + 32p^4 \cos(2r) - 64\mu p^4 \cos(2r) + 32\mu^2 p^4 \cos(2r) - p \cos(4r) \\
& + 2\mu p \cos(4r) + 5p^2 \cos(4r) - 10\mu p^2 \cos(4r) + 4\mu^2 p^2 \cos(4r) \\
& - 8p^3 \cos(4r) + 16\mu p^3 \cos(4r) - 8\mu^2 p^3 \cos(4r) \\
& + 4p^4 \cos(4r) - 8\mu p^4 \cos(4r) + 4\mu^2 p^4 \cos(4r) \\
& \pm 8\sqrt{2} \sqrt{\left(\begin{aligned} & ((-1 + \mu)^2(-1 + p)^3 p^3 \cos^2 r(-5 + 2\mu - 12p + 24\mu p \\ & - 12\mu^2 p + 12p^2 - 24\mu p^2 + 12\mu^2 p^2 \\ & + 4(1 - 4(-1 + \mu)^2 p + 4(-1 + \mu)^2 p^2) \cos(2r) \\ & + ((1 - 2p)^2 - 2\mu(1 - 2p)^2 + 4\mu^2(-1 + p)p) \cos(4r) \end{aligned} \right)}
\end{aligned} \tag{22}$$

The eigen values of $\rho_f^{\text{Pf}} \tilde{\rho}_f^{\text{Pf}}$ are given as under

$$\begin{aligned}\lambda_1 &= (1 + 2(-1 + \mu)p - 2(-1 + \mu)p^2)^2 \cos^2 r \\ \lambda_2 &= 4(-1 + \mu)^2(-1 + p)^2 p^2 \cos^2 r \\ \lambda_{3,4} &= 0\end{aligned}\tag{23}$$

The concurrence C , is calculated using equation (18). It can be easily checked from equations (20-23) that the concurrence becomes $\cos r$ if we set $p = \mu = 0$, which reproduces the results of Ref. [4]. Similarly the results of Ref [10-11] can be reproduced by setting $\mu = 0$.

III. DISCUSSIONS

We have computed the mathematical relations for concurrence in case of amplitude damping, depolarizing, phase flip and bit-phase flip channels. However, due to very lengthy mathematical expressions, we have only plotted it for different parameters such as p , r , μ respectively.

In figures 1 and 2, we plot the concurrence as a function of memory parameter μ for different values of Rob's acceleration, r for decoherence parameter $p = 0.5$ for amplitude damping, depolarizing channels respectively. In figures 3 and 4, we plot the concurrence as a function of memory parameter μ with others parameters similar as in figures 1 and 2 for bit-phase flip and phase flip channels respectively. It is seen that quantum memory enhances the entanglement of Dirac fields in contrast to the effect of decoherence. It is also seen that the depolarizing channel influences the entanglement more heavily in comparison to the other channels. The depolarizing channel enhances the degree of entanglement upto 1 even with 50% decoherence (see figure 2). It is clear from figure 3 that for lower values of memory parameter, the decoherence dominates and ESD behaviour can be seen. However for higher values of memory, the ESD can also be avoided for flipping channels (see figures 3 and 6).

In figure 5, we plot the concurrence as a function of Rob's acceleration r for $p = \mu = 0.5$ for amplitude damping, depolarizing, bit-phase flip and phase flip channels. It is seen that the entanglement degradation is controlled due to the presence of quantum memory even at 50% decoherence. It is also seen that entanglement is heavily degraded by amplitude damping channel as compared to other channels. In figure 6, we plot the concurrence as a function of decoherence parameter p for $\mu = 0.5$ and $r = \pi/6$ for amplitude damping, depolarizing, bit-phase flip and phase flip channels. It is seen that the maximum entanglement degradation occurs for amplitude damping channel as compared to other channels. Furthermore, the symmetric behaviour of flipping

channels is seen with maximum degradation for 50% decoherence. In order to check the validity of our calculations, we plot in figure 7, the concurrence as a function of decoherence parameter p for $\mu = 0$ and $r = \pi/10$ for amplitude damping, depolarizing, bit-phase flip and phase flip channels. It is seen that the maximum entanglement degradation occurs for bit-phase flip channel as compared to other channels. It is clear from the figure that the graphs of Ref. [10, 11] are reproduced in the absence of memory.

IV. CONCLUSIONS

We study the effect of quantum memory in non-inertial frames for amplitude damping, depolarizing, phase flip and bit-phase flip channels. It is shown that the entanglement of initial state is heavily influenced by quantum correlations. It is seen that quantum memory compensates the loss of entanglement generated by the Unruh effect and decoherence. It is interesting to note that the sudden death of entanglement disappears for any acceleration for higher degree of memory. Furthermore, the entanglement of Dirac fields increases as we increase the degree of memory. In conclusion, we can say that quantum memory can avoid ESD caused by Unruh effect for all the channels considered.

-
- [1] P. M. Alsing and G. J. Milburn, Phys. Rev. Lett. **91**, 180404 (2003).
 - [2] A. Peres, P. F. Scudo, and D. R. Terno, Phys. Rev. Lett. **88**, 230402 (2002).
 - [3] R. M. Gingrich and C. Adami Phys. Rev. Lett. **89**, 270402 (2002).
 - [4] P.M. Alsing, I. Fuentes-Schuller, R. B.Mann, and T. E. Tessier, Phys. Rev. A **74**, 032326 (2006).
 - [5] Q. Pan and J. Jing, Phys. Rev. A **77**, 024302 (2008); Phys. Rev. D **78**, 065015 (2008).
 - [6] J. Wang, Q. Pan, Songbai Chen, and Jiliang Jing, Phys. Lett. B **677**, 186 (2009).
 - [7] J. Wang, J. Deng, and J. Jing, Phys. Rev. A **81**, 052120 (2010).
 - [8] L. Lamata, M. A. Martin-Delgado, and E. Solano, Phys. Rev. Lett. **97**, 250502 (2006).
 - [9] I. Fuentes-Schuller and R. B. Mann, Phys. Rev. Lett. **95**, 120404 (2005).
 - [10] J. Wang and J. Jing, Phys. Rev. A **82**, 032324 (2010) .
 - [11] S. Khan and M. K. Khan, J. Phys. A: Math. Theor. **44**, 045305 (2011).
 - [12] C. Macchiavello and G. M. Palma, Phys. Rev. A, **65**, 050301 (2002).
 - [13] Y. Yeo and A. Skeen, Phys. Rev. A, **67**, 064301 (2003).
 - [14] V. Karimipour, et. al., Phys. Rev. A, **74**, 062311 (2006).
 - [15] G. Bowen, S. Mancini, Phys. Rev. A, **69**, 01236 (2004).

- [16] D. Kretschmann, R. F. Werner, *Phys. Rev. A*, **72**, 062323 (2005).
- [17] M. A. Nielsen and I. L. Chuang, *Quantum Computation and Quantum Information* (Cambridge: Cambridge University Press, 2000)
- [18] W. K. Wootters, *Phys. Rev. Lett.* **80**, 2245 (1998).

Figures captions

Figure 1. The concurrence is plotted as a function of memory parameter μ for different values of Rob's acceleration, $r = 0$ (solid line), $r = \pi/6$ (dashed line) and $r = \pi/4$ (dotted line) for decoherence parameter $p = 0.5$ for amplitude damping.

Figure 2. The concurrence is plotted as a function of memory parameter μ for different values of Rob's acceleration, $r = 0$ (solid line), $r = \pi/6$ (dashed line) and $r = \pi/4$ (dotted line) for decoherence parameter $p = 0.5$ for depolarizing channel.

Figure 3. The concurrence is plotted as a function of memory parameter μ for different values of Rob's acceleration, $r = 0$ (solid line), $r = \pi/6$ (dashed line) and $r = \pi/4$ (dotted line) for decoherence parameter $p = 0.5$ for bit-phase flip channel.

Figure 4. The concurrence is plotted as a function of memory parameter μ for different values of Rob's acceleration, $r = 0$ (solid line), $r = \pi/6$ (dashed line) and $r = \pi/4$ (dotted line) for decoherence parameter $p = 0.5$ for phase flip channel.

Figure 5. The concurrence is plotted as a function of Rob's acceleration r for $p = \mu = 0.5$ for amplitude damping (solid line), depolarizing (dashed line), bit-phase flip (dotted line) and phase flip (dot dashed line) channels.

Figure 6. The concurrence is plotted as a function of decoherence parameter p for $\mu = 0.5$ and $r = \pi/6$ for amplitude damping (solid line), depolarizing (dashed line), bit-phase flip (dotted line) and phase flip (dot dashed line) channels.

Figure 7. The concurrence is plotted as a function of decoherence parameter p for $\mu = 0$ and $r = \pi/10$ for amplitude damping (solid line), depolarizing (dashed line), bit-phase flip (dotted line) and phase flip (dot dashed line) channels.

Table Caption

Table 1. Single qubit Kraus operators for amplitude damping, depolarizing, bit-phase flip and phase flip channels where p represents the decoherence parameter.

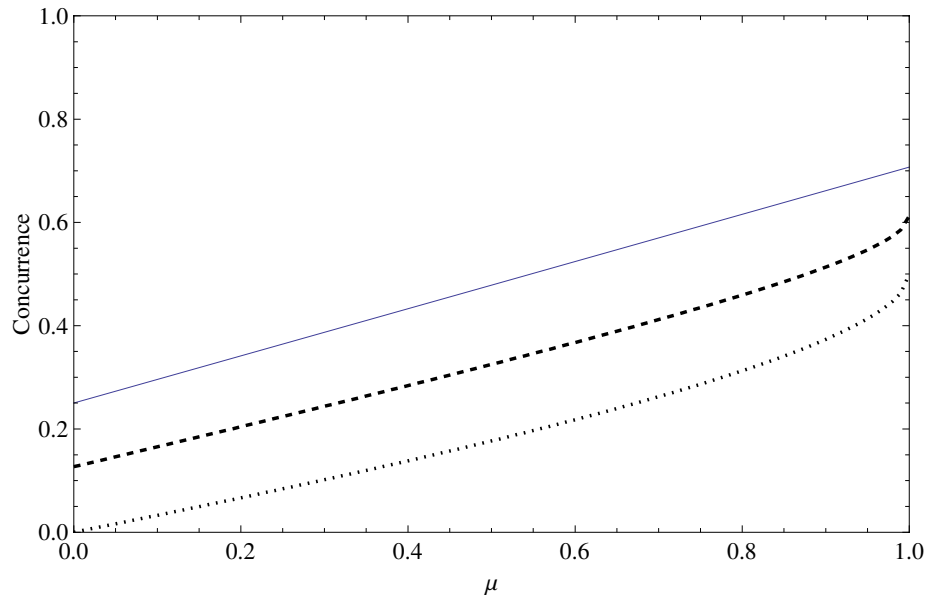


FIG. 1: The concurrence is plotted as a function of memory parameter μ for different values of Rob's acceleration, $r = 0$ (solid line), $r = \pi/6$ (dashed line) and $r = \pi/4$ (dotted line) for decoherence parameter $p = 0.5$ for amplitude damping.

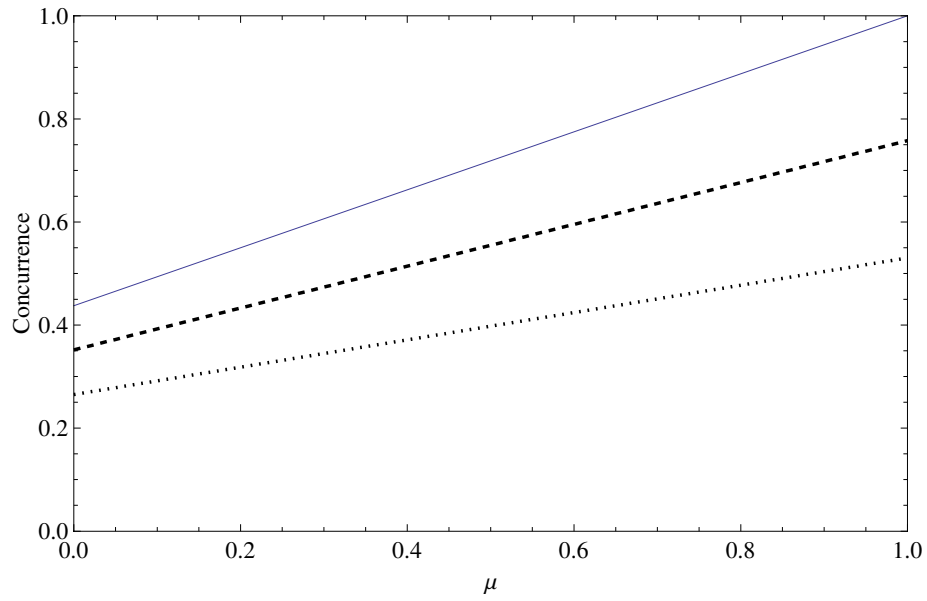


FIG. 2: The concurrence is plotted as a function of memory parameter μ for different values of Rob's acceleration, $r = 0$ (solid line), $r = \pi/6$ (dashed line) and $r = \pi/4$ (dotted line) for decoherence parameter $p = 0.5$ for depolarizing channel.

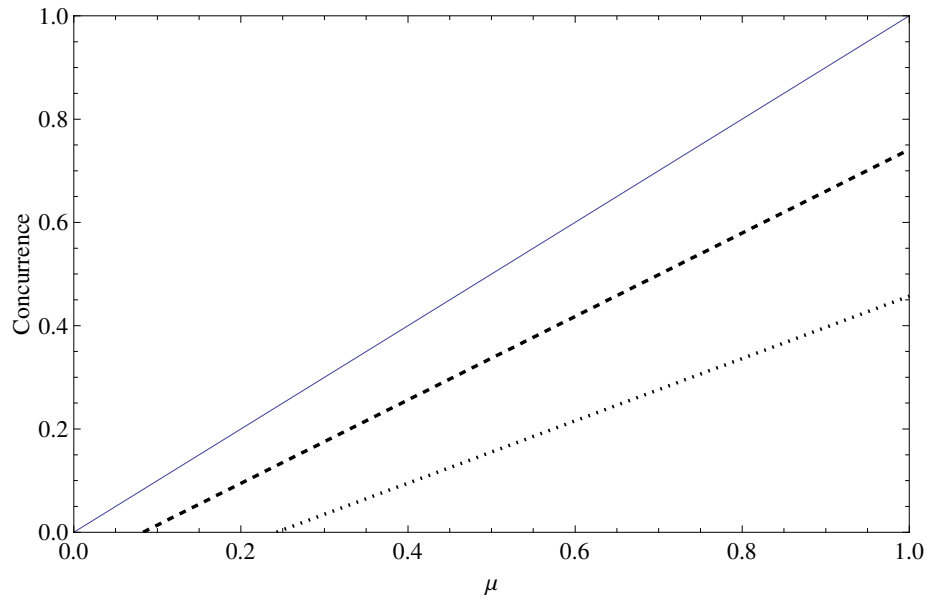


FIG. 3: The concurrence is plotted as a function of memory parameter μ for different values of Rob's acceleration, $r = 0$ (solid line), $r = \pi/6$ (dashed line) and $r = \pi/4$ (dotted line) for decoherence parameter $p = 0.5$ for bit-phase flip channel.

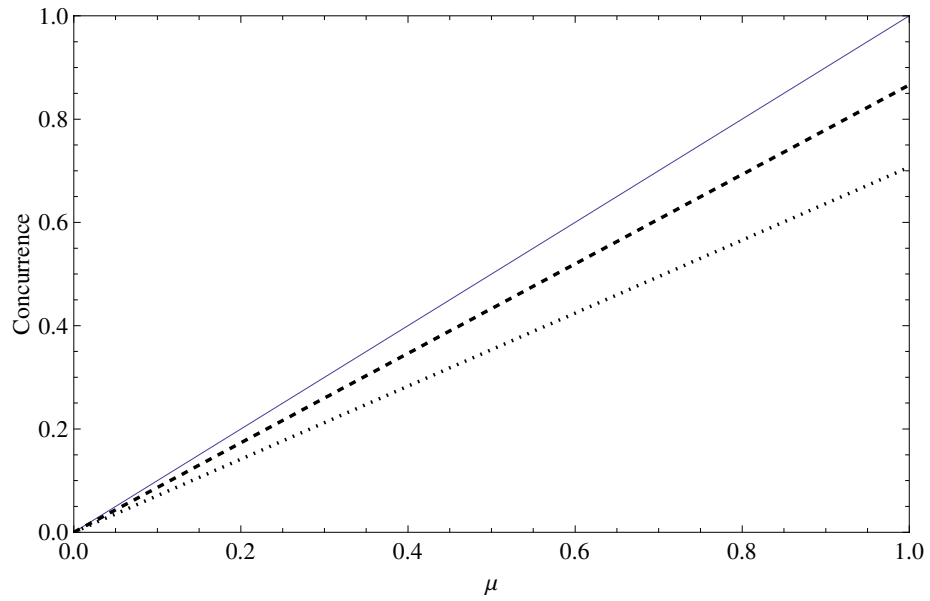


FIG. 4: The concurrence is plotted as a function of memory parameter μ for different values of Rob's acceleration, $r = 0$ (solid line), $r = \pi/6$ (dashed line) and $r = \pi/4$ (dotted line) for decoherence parameter $p = 0.5$ for phase flip channel.

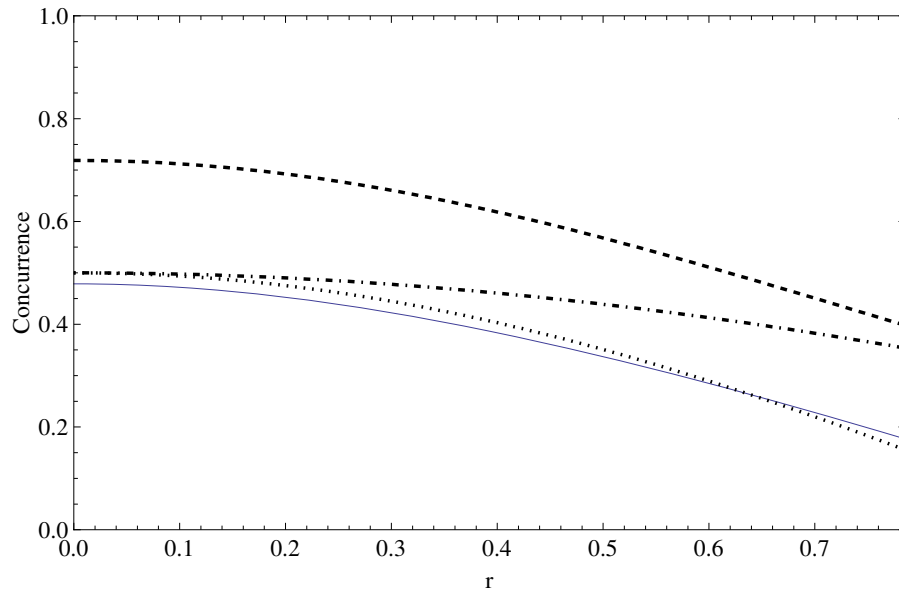


FIG. 5: The concurrence is plotted as a function of Rob's acceleration r for $p = \mu = 0.5$ for amplitude damping (solid line), depolarizing (dashed line), bit-phase flip (dotted line) and phase flip (dot dashed line) channels.

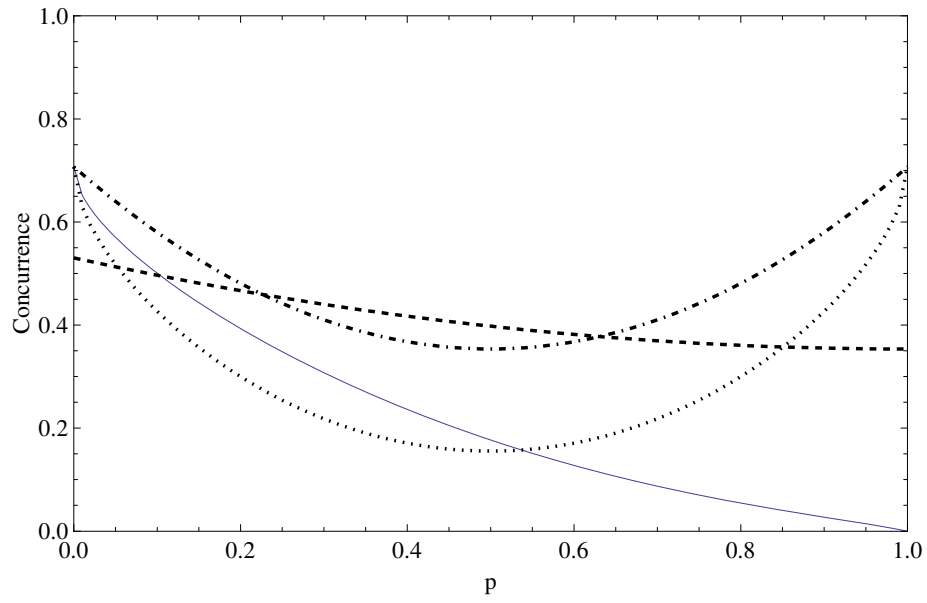


FIG. 6: The concurrence is plotted as a function of decoherence parameter p for $\mu = 0.5$ and $r = \pi/6$ for amplitude damping (solid line), depolarizing (dashed line), bit-phase flip (dotted line) and phase flip (dot dashed line) channels.

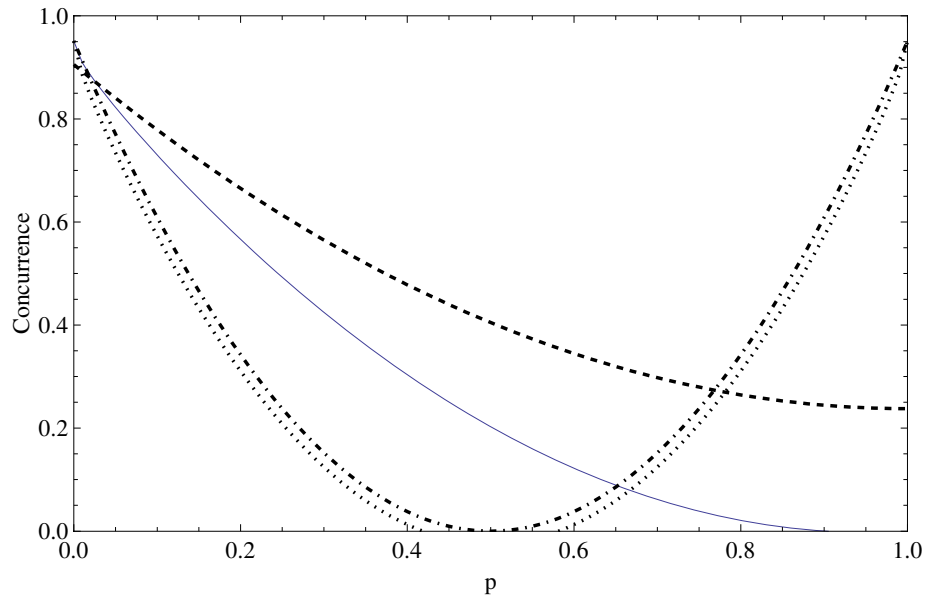


FIG. 7: The concurrence is plotted as a function of decoherence parameter p for $\mu = 0$ and $r = \pi/10$ for amplitude damping (solid line), depolarizing (dashed line), bit-phase flip (dotted line) and phase flip (dot dashed line) channels.

TABLE I: Single qubit Kraus operators for amplitude damping, depolarizing, bit-phase flip and phase flip channels where p represents the decoherence parameter.

Amplitude damping channel	$A_0 = \begin{bmatrix} 1 & 0 \\ 0 & \sqrt{1-p} \end{bmatrix}, A_1 = \begin{bmatrix} 0 & \sqrt{p} \\ 0 & 0 \end{bmatrix}$
Depolarizing channel	$A_0 = \sqrt{1 - \frac{3p}{4}}I, A_1 = \sqrt{\frac{p}{4}}\sigma_x$ $A_2 = \sqrt{\frac{p}{4}}\sigma_y, A_3 = \sqrt{\frac{p}{4}}\sigma_z$
Bit-phase flip channel	$A_0 = \sqrt{1-p}I, A_1 = \sqrt{p}\sigma_y$
Phase flip channel	$A_0 = \sqrt{1-p}I, A_1 = \sqrt{p}\sigma_z$